

A study of high-index-contrast 90° waveguide bend structures

R. L. Espinola, R. U. Ahmad, F. Pizzuto, M. J. Steel and R. M. Osgood, Jr.

Microelectronics Sciences Laboratories, Columbia University, New York, NY 10027 USA

rl7@columbia.edu, rokan@cumsl.ctr.columbia.edu

<http://cumsl.ctr.columbia.edu/>

Abstract: We present an evaluation of the parameters involved in designing low-loss right-angle waveguide bends based on a high index contrast materials system. We apply the finite difference time domain method (FDTD) to several two-dimensional bend structures and study the effects of varying the bend geometry. Such a study is relevant for the understanding of bend mechanisms and for the optimization and fabrication of high-density high-contrast integrated optical components. The study indicates that high bend transmission can be achieved with the addition of a low- Q resonant cavity; however, similar or even better performance can be achieved with a structure that combines a corner mirror with a phase retarder. The use of a double corner mirror structure is shown to further increase the bend transmission, with little increase in bend area.

© 2001 Optical Society of America

OCIS codes: (130.0130) Integrated optics; (220.0220) Optical design and fabrication

References and links

1. M. Naydenkov and B. Jalali, "Advances in silicon-on-insulator photonic integrated circuit (SOIPIC) technology," in *IEEE International SOI Conference*, (Institute of Electrical and Electronics Engineers, Piscataway, NJ, 1999), pp. 56-66.
2. H. Nishihara, M. Haruna, and T. Suhara, *Optical Integrated Circuits*, (McGraw Hill, New York, NY 1989).
3. P. Buchmann and H. Kaufmann, "GaAs Single-Mode Rib Waveguides with Reactive Ion-Etched Totally Reflecting Corner Mirrors," *J. Lightwave Technol.* **LT-3**, 785-788 (1985).
4. W. Yang and A. Gopinath, "Design of planar optical waveguide corners with turning mirrors," in *Proceedings of Integrated Optics*, Technical Digest Series, Vol. 6 (Optical Society of America, Washington, D.C., 1996), pp. 58-63.
5. Y. Chung and N. Dagli, "Experimental and theoretical study of turning mirrors and beam splitters with optimized waveguide structures," *Opt. and Quantum Electron.* **27**, 395-403 (1995).
6. A. Mekis, J. C. Chen, I. Kurland, S. Fan, P. R. Villeneuve, and J. D. Joannopoulos, "High transmission through sharp bends in photonic crystal waveguides," *Phys. Rev. Lett.* **77**, 3787-3790 (1996).
7. R. D. Meade, A. Devenyi, J. D. Joannopoulos, O. L. Alerhand, D. A. Smith, and K. Kash, "Novel applications of photonic band gap materials: Low-loss bends and high Q cavities," *J. Appl. Phys.* **75**, 4753-4755 (1994).
8. S-Y. Lin, E. Chow, V. Hietala, P. R. Villeneuve, and J. D. Joannopoulos, "Experimental demonstration of guiding and bending of electromagnetic waves in a photonic crystal," *Science* **282**, 274-276 (1998).
9. T. Baba, N. Fukaya, and J. Yonekura, "Observation of light propagation in photonic crystal optical waveguides with bends," *Electronics Lett.* **35**, 654-655 (1999).
10. C. Manolatou, S. G. Johnson, S. Fan, P. R. Villeneuve, H. A. Haus, J. D. Joannopoulos, "High-density integrated optics," *J. Lightwave Technol.* **17**, 1682-1692 (1999).
11. H. A. Haus, *Waves and Fields in Optoelectronics*, (Prentice-Hall, Englewood Cliffs, NJ. 1984).

12. E. G. Neumann, "Reducing radiation loss of tilts in dielectric optical waveguides," *Electronics Lett.* **3**, 369-371 (1986).
 13. FullWAVE, RSoft Inc. Research Software, <http://www.rsoftinc.com>.
 14. J. P. Berenger, "A perfectly matched layer for the absorption of electromagnetic waves," *J. Comp. Phys.*, **114**, 185-200 (1994).
 15. B. E. Little, J. S. Foresi, G. Steinmeyer, E. R. Thoen, S. T. Chu, H. A. Haus, E. P. Ippen, L. C. Kimmerling, W. Greene, "Ultra-Compact Si-SiO₂ Microring Resonator Optical Channel Dropping Filters," *Phot. Tech. Lett.* **10**, 549-551 (1998).
 16. M. Cai, G. Hunziker, K. Vahala, "Fiber-Optic Add-Drop Device Based on a Silica Microsphere-Whispering Gallery Mode System," *Phot. Tech. Lett.* **11**, 686-687 (1999).
-

1 Introduction

High-density photonic circuits have recently become of interest because of the growing demand for low-cost, highly-functional optical chips. In general, practical designs require a material system with relatively high refractive index contrast in order to increase the packing density of the optical elements [1]. In addition, high density also requires the use of sharp, e.g. 90°, bends. However, low-loss sharp bends cannot be easily achieved with standard waveguide technology because waveguide loss increases exponentially with the inverse bend radius [2]. As a result, several new approaches to achieving 90°-bends have recently been described including the use of photonic crystals, corner mirrors, and waveguide resonators. While certain types may be hard to fabricate, each of the techniques is predicted to allow sharp bends with low loss.

For example, the conventional approach to 90°-bend structures is the use of waveguide corner mirrors, which exploit strong modal confinement and total internal reflection (TIR) at the corner [3, 4]. With suitable mirror placement and angle, these structures can reflect the incident light with low-loss in the bend. In one implementation, the excess radiation loss on 90°-bends was ~0.8 dB/mirror and ~1.0 dB/mirror for quasi-TE and quasi-TM modes, respectively [5].

More recently, the use of photonic crystal waveguides has been proposed for making high transmission 90°-bends [6]. In this case, photonic band-gap (PBG) materials are modified by inserting a line of defects that can support a localized mode having a frequency located within the gap [7]. The defect line thus supports a local state and acts as a waveguide. For example, by using a 2D photonic crystal of dielectric rods in air and removing rods to form a 90°-bend, experiments in the microwave regime demonstrated a transmission of about 80% [8]. Recent experiments with similar structures in the optical region have also been encouraging, although their fabrication remains challenging [9].

Finally, Manolatou *et al.* [10] have proposed the addition of a resonant cavity on the inside corner of a bend to enhance the performance of 90°-bends using high-index-contrast waveguides [see Fig. 1(a) and Fig. 1(b)]. The design is inspired by the principle of weakly coupled resonators, which predicts that a symmetric resonator with four ports can couple an incoming channel to an outgoing channel without reflection [11]. Here the input and output waveguides correspond to the four ports (forward and backward-traveling modes in each of the two arms) with the enlarged cavity being the resonator having a square side. In their numerical experiments, Manolatou *et al.* obtained a simulated transmission of over 98% and a bandwidth of more than 120 nm [10]. Their work also showed that for a *strongly* coupled low- Q resonator, one can still extract virtually all the energy, just as for the weakly coupled case. Thus the resonator argument apparently remains qualitatively valid despite the fact that the resonators are not weakly coupled [10].

Figure 1(b) shows an alternative to the original proposal of a simple symmetric resonator; it uses a "folded" 45° resonator and, as for the rectangular resonator in Fig. 1(a), it also utilizes a strongly coupled low- Q resonant cavity. The device has a

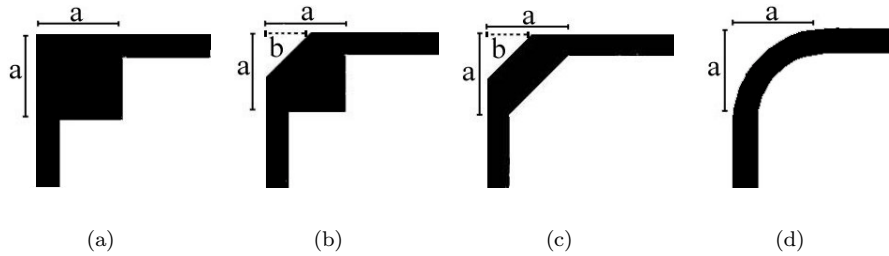


Fig. 1: Schematics of bend designs that were studied. The characteristic dimensions a and b are used as variables in the designs below.

square side, a , and a 45° cut depth, b . In this configuration a traveling mode undergoes total internal reflection at the 45° surface and is guided around the modified corner by the outer walls; see discussion section 3, below. Although the additional high index material inside the bend preserves the function of a resonant cavity, it can also be viewed as a phase retarder. Phase retarders, which were originally proposed by Neumann, use a design in which the added index material on the inside corner of an abrupt bend reduces the local phase velocity of the inner wavefronts as compared to the outer, thereby causing the light to turn [12]. Therefore, upon a closer inspection of the structure in Fig. 1(b), it might be argued that, aside from any resonant cavity effects, the transmission is improved simply through high-index guiding via a conventional corner mirror. It is thus difficult to evaluate the relative importance of the cavity as compared to the other guiding mechanisms without a more extensive study. Also, it is of particular interest to determine whether it is possible to attain similar results through a simpler design, such as a modified corner mirror, an example of which is shown in Fig. 1(c).

In this paper, we perform a comparative study of the relative merits of the approaches to designing bend structures shown in Figs. 1(b–d), using a series of finite difference time domain simulations. Specifically, the goal is to study the central factors leading to the performance of 90° -bends. In Section 2, we describe the numerical method and simulation parameters used in order to solve the 2-D structures. Next, in Section 3, we examined the isolated-resonator contribution to the bend by varying the resonator placement. For comparison in Section 4, we study the isolated index-guiding contribution of the corner mirror by varying the mirror widths. The results of both studies can help provide a better understanding of the different factors involved in designing and optimizing 90° -bends.

2 Overview of Study and Numerical Method

The study consisted of comparisons of index-guided 90° -bend geometries using resonator, corner mirror, and a simple bend, or their combinations. A series of resonator placements and corner mirror sizes were optimized and examined using a commercial FDTD tool [13] to simulate the 2-D bend structures. In several cases, computational accuracy was also cross-checked by comparison to similar calculations using time-domain beam propagation. For all structures, the input and output guides had widths of $0.2 \mu\text{m}$ and refractive index $n=3.2$ surrounded by air. The values were chosen in order to ensure single-mode operation over the entire bandwidth of excitation and to closely match the refractive index of a practical material system such as AlGaAs. The simulations assume TE polarization with the computational domain employing an FDTD cell size of 10 nm, terminated by Perfectly Matched Layer (PML) Boundaries [14]. We used 5 fs wide Gaussian-pulse inputs of the fundamental mode of the waveguide at $\lambda=1.55 \mu\text{m}$

and also used CW inputs to check the accuracy at the longer wavelengths. Accuracy checking of the Gaussian-pulse method was necessary since the pulsed method assumes the same input modeshape for all frequencies in the simulation when there are, in fact, differences in the modal field at each frequency. Therefore, we used as input the correct modeshape in the CW simulations to ascertain that this assumption did not lead to significant error. The accuracy of the simulations was further confirmed by reducing the spatial and temporal grid steps, as well as by comparison of known structures with published results. Note that all of the figures presented in this paper use the accurate CW data. The basic quantity examined is the fraction of input power coupled into the fundamental mode of the output guide as a function of wavelength for each bend structure; our goal was to optimize that value.

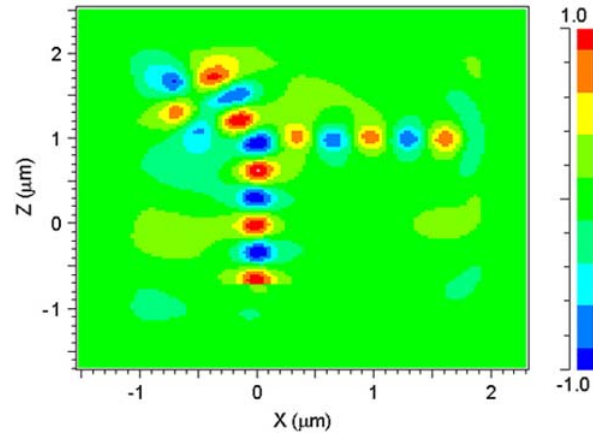
3 Roles of Resonator and Index-Guiding

This section, we evaluate the relative importance of cavity resonance on the bend performance of the resonators shown in Fig. 1(a), and by an analogy, Fig. 1(b). We accomplish this via a systematic study of the resonator performance via the placement of the input/output port of the resonator cavity. The optical properties of the resonator of Fig. 1(a) can be discussed keeping in mind the well known physics of microring and microsphere resonators. These devices utilize whispering gallery modes (WGM) that are coupled to input and output ports [15, 16]. There are, of course, important differences between our structure and these high- Q resonators. For example, the input/output waveguides used here have much stronger coupling. In addition, the orientation of the input and output ports are somewhat different from those typically used in circular resonators. Finally, the resonators used in our study have relatively low- Q 's, estimated to be between 13 and 30 [10]. Despite these differences, each of the structures has an input/output port and stores significant amounts of optical energy, just as in high- Q resonator devices. Because of this analogy to circular resonators, we anticipate that the bend resonator will have cavity standing waves or modes, accompanied by traveling modes of the waveguide. The low- Q of the cavity will cause *both* the standing and the traveling modes to determine their optical performance.

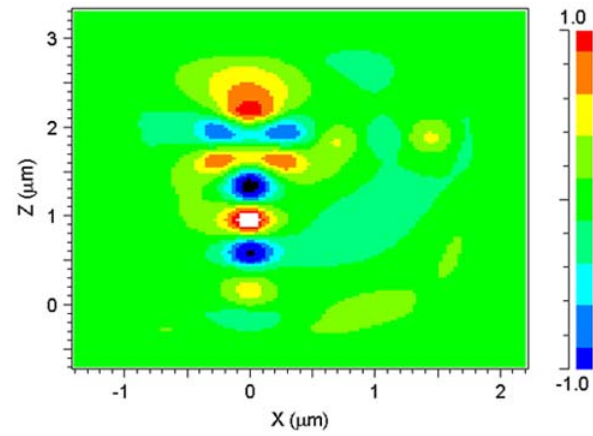
In addition to the effect of the cavity resonance, the geometry of the structures will affect the traveling waves through the mechanism of index-guiding [12]. Several studies have shown that judiciously placed dielectric features can greatly enhance guiding of a waveguide mode when it encounters a bend. The efficacy of this index-guiding mechanism is expected to be highly dependent on the placement of dielectric features [12].

Intuitively we also expect that a variation in placement of the input and output guides will cause a different proportion of traveling-wave versus the standing-wave resonator modes. Furthermore, placing the cavity at the outer, center and inner side of the bend intersection with respect to the input and output ports should cause a change in this proportion. In fact, these effects can be seen clearly in field amplitudes obtained in a series of FDTD simulations for these three input/output waveguide positions.

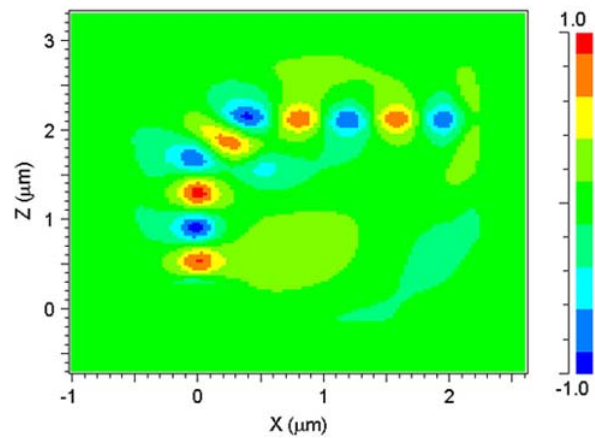
In particular, Figs. 2(a-c), show the field outputs of the three resonator placements using CW input operating at the wavelengths of peak transmission according to Fig. 3. The cavities having the outer and inner placements cause the light to excite these traveling waveguide modes that can be regarded as WGM that rotate either clockwise (inner placement) or counter-clockwise (outer placement) into the output port of the bend. Since the outer placement in Fig. 2(a) increases the index on the outside corner of the bend, the added index retards the outer wave fronts [12], acting as an inverse phase retarder so as to excite an acceptable WGM that rotates counterclockwise through the cavity and to the output guide. The cavity placed inside the bend (Fig. 2(c)) acts as a phase retarder for the inner wave front and helps the phase front to turn clockwise



(a) outer placement



(b) central placement



(c) inner placement

Fig. 2: Field output for the three placements, outer, central, and inner, for input/output waveguides on a square resonator.

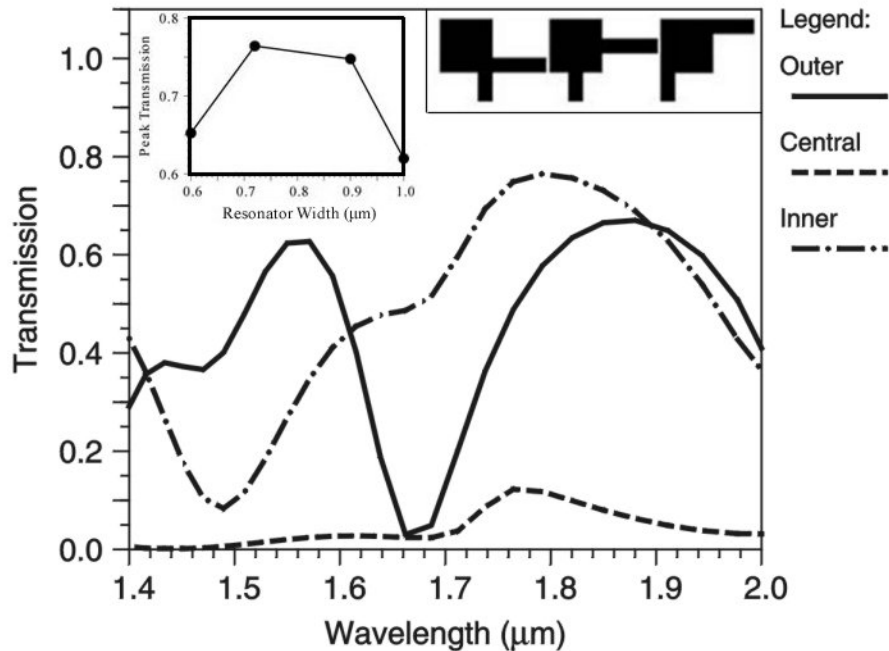


Fig. 3: Transmission spectra of the square cavity corresponding to three positions of the input/output waveguides. The right inset shows the three different positions used to generate the three plots. The left inset shows an example of optimization of the cavity size for the inner placement of the waveguides.

directly onto the output arm. This effect would be expected to yield high performance. On the other hand, a symmetric cavity, such as obtained with the central placement (Fig. 2(b)), does not provide phase-retardation either to the inner or to the outer wave front. Thus, as seen in Fig. 2(b), the central placement provides no circular whispering gallery mode for the light. Instead, the light couples into a symmetric standing cavity mode that is much smaller in amplitude than the traveling mode and largely reflects directly back into the input port.

With this intuitive picture in mind, a quantitative assessment for each of the input/output waveguide placements was obtained by using FDTD simulation to calculate the transmitted light power for each of the three cavities shown above. Also, since one would anticipate that the optimum position of the output port would depend on the cavity-resonance conditions, simulation experiments were carried out over a series of cavity-resonator dimensions. As a result, the design was optimized for the maximum peak transmission with respect to the cavity size, i.e. the side of the square resonator in micrometers, at each test wavelength; thus Fig. 3 shows only the spectra of the optimum for each placement in the figure. One example of this optimization process for the inner-placed cavity is shown in the left inset. As shown in Fig. 3 and as expected from the intuitive discussion above, the central placement tends to suppress index-guiding and consequently produces the lowest performance. The maximum transmission for this resonator placement is well below 0.2 over the entire spectral region. On the other hand, the inner placement of the square cavity provides the maximum transmission of 0.76 at $\lambda=1.79 \mu\text{m}$ and has well defined resonance peaks. The transmission of the cavity with the outer placement has a lower maximum transmission, presumably because of lossy scattering at the corners of the cavity. Note that in this configuration, light has to undergo a 270° counter-clockwise rotation as opposed to the 90° clockwise rotation

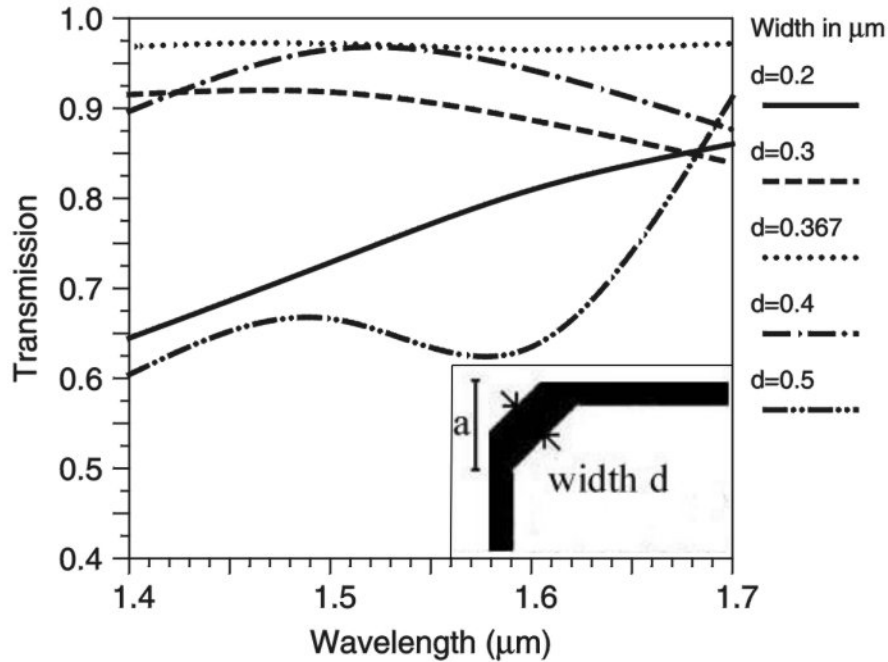


Fig. 4: Variation of the corner mirror width. Five mirrors are considered, from 0.2-0.5 μm in width, as indicated in the legend.

of the inner placement.

These results confirmed our expectations that the bend performance is dependent on the placement of the resonant cavity; thus the results are consistent with the importance of exciting traveling wave modes. In addition, there is a strong contribution from index-guiding to the overall transmission of these resonant cavity structures. Note that in most discussions of resonant cavities, which are framed in terms of coupled-mode theory, the contribution of cavity placement is not explicitly considered. However, as clearly shown in Fig. 3 and Fig. 2, the placement of the input/output waveguide in these bend structures does affect the excitation of useful cavity modes. In fact, it is obvious that in the strong coupling regime, the details of the coupling between the ports and the resonator determine which modes get excited; the placement of the cavity, therefore, has an important effect on performance. Lastly, the best performance is achieved with the inner placement of the resonator since it adds a phase retarder for the inner wave front. In this case, phase retardation contributes significantly to achieving the high transmission.

4 Corner Mirror Design

The previous section showed that index-guiding offers an important contribution to the overall performance of a resonator bend. This suggests that the resonator-bend structure might be modified even further to optimize transmission. In this connection, consider the mirror-folded resonator shown in Fig. 1(b), that is, a resonator composed of a corner mirror and an “inner-placed” resonator. This device also resembles a corner mirror with an inner high-index region. In fact, since the resonator has a relatively low Q and since index guiding was found to play such an important role in the studies of the previous section, it might be argued that resonator effects would be unimportant for this device. Thus a study of a simpler corner mirror design, without a resonator, was undertaken.

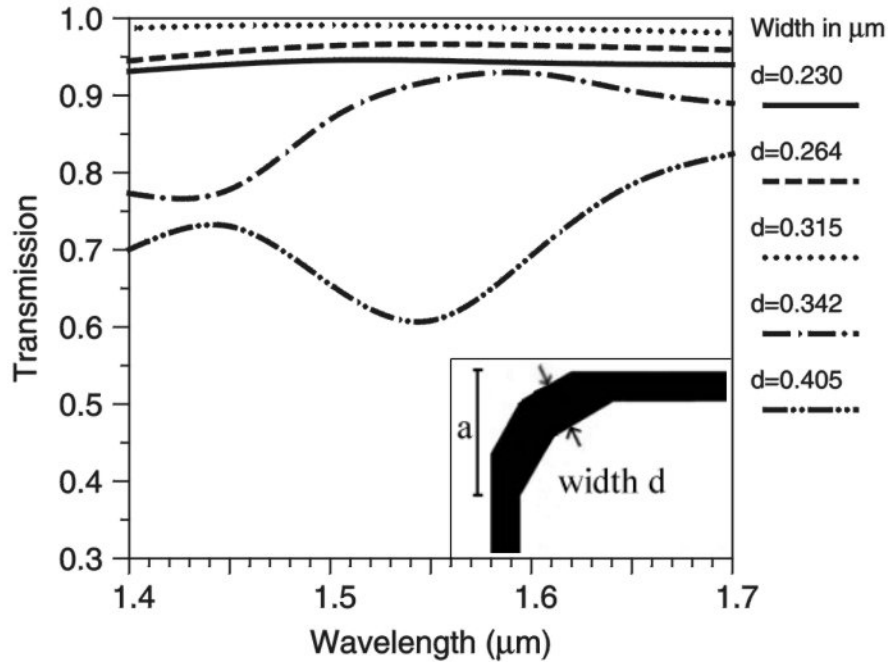


Fig. 5: Variation of the double mirror width. Five mirrors are examined, from 0.230–0.405 μm in width.

In fact, rather than incorporating complex designs and other guiding mechanisms, it is worth investigating whether a simple variation in the width and geometry of the corner mirror (see Fig. 1(c)) can lead to the same high transmission characteristics as the basic square-resonator bend. Our design process started with the cut resonator shown in Fig. 1(b) [10]. The cavity region was reduced to the point that it was basically a 45°-bend waveguide segment, with a fixed 45° depth “cut”, $b=0.42 \mu\text{m}$ (see Fig. 1), and a uniform width, d , of 0.2 μm . Then, as described above, the width of the corner mirror region, d , was varied from 0.2–0.5 μm , while keeping $b=0.42 \mu\text{m}$, in order to find an optimum width. In terms of device “layout”, a mirror characterized by a dimension a uses a device area of a resonator also of dimension a or a conventional circular bend of radius a (Fig. 1(d)). The results of the variation in d are shown in Fig. 4.

The results also show that, in these high-index-contrast structures, the corner mirror region does not have to be significantly wider than the waveguides themselves. In particular, the transmission of the mirror is maximum at a mirror width comparable to that of the waveguide. Thus, an increase in the mirror width was found to yield a steady increase in the transmission around the wavelength of interest, namely $\lambda=1.55 \mu\text{m}$, to a maximum value of 0.968 at a width of $d=0.367 \mu\text{m}$ corresponding to a bend factor of $a=0.74 \mu\text{m}$. This value of d is ~ 1.5 times the waveguide width. This improvement can be explained by the additional phase retardation of the inner wavefronts and the optimized geometry of the corner mirror. Although a slightly wider bend with a width of $d=0.4 \mu\text{m}$ gave a similar peak transmission at $\lambda=1.55 \mu\text{m}$, the wavelength response was not as flat and had a smaller bandwidth over the optimum design. Further widening of the mirror region, e.g. $d=0.5 \mu\text{m}$, as seen in Fig. 4, resulted in general deterioration of the transmission spectrum and a nonuniform response, presumably because of the increased contribution of high-order modes excited that were unable to efficiently couple into the output arm. In general however, simulations showed a low light intensity

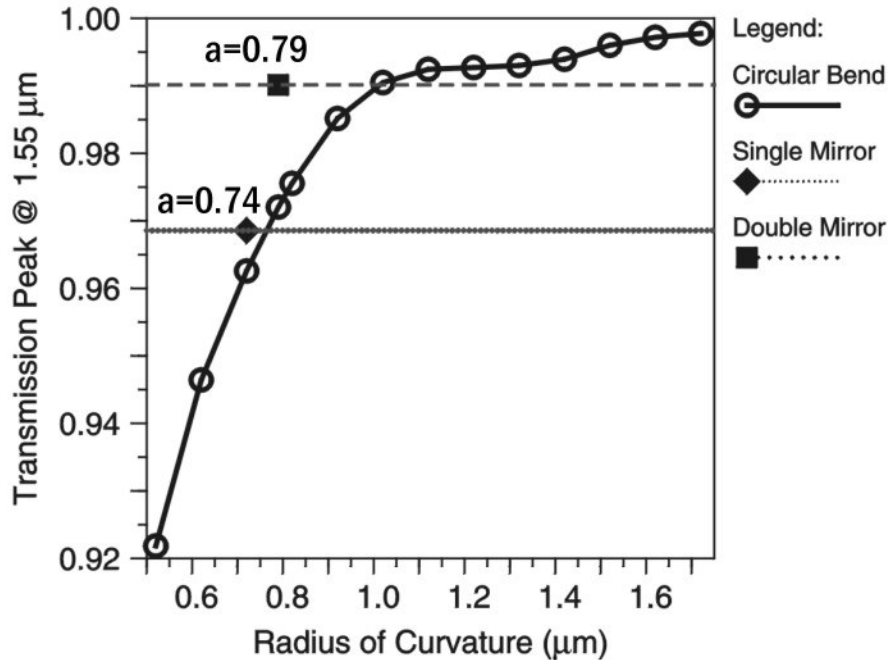


Fig. 6: Transmission spectrum of the circular bend at $\lambda=1.55 \mu\text{m}$ versus the bend radius of curvature. In addition, peak transmission values of the optimized double ($a=0.79\mu\text{m}$) and single mirror ($a=0.74\mu\text{m}$) bend are shown for comparison.

“leaking” from sharp bend intersections. Since the waveguide bends were modeled with ideal waveguide parameters, this loss must have originated from mode-conversion and radiation at the sharp corners.

The relatively high performance of the mirror-like structure and the fact that there is loss arising from the sharp intersections suggest further improvements in the performance of the corner mirror, albeit with a slight increase in overall design complexity. The improvements involve replacing the corner mirror by a double mirror as shown in the inset of Fig. 5. In order to optimize the transmission of this double mirror, we varied the width from $0.230\text{-}0.405 \mu\text{m}$. This process gave us an optimum width of $d=0.315 \mu\text{m}$, corresponding to $a=0.79 \mu\text{m}$. We were then able to achieve a reasonably flat transmission spectra with a transmission of 0.99 at a wavelength of $\lambda=1.55 \mu\text{m}$; see Fig. 5. Increasing the bend width beyond the optimum point gave a structure with a nonuniform response and poor transmission because of excitation of high-order modes that then inefficiently coupled into the output arm. Although the increase in peak transmission is presumably because of the less abrupt junction for the double mirror structure, a further increase in the number of segments of the mirror was found to monotonically decrease the peak transmission within the overall bend dimensions, i.e. the optimized bend factor, a . While it is also possible to use a conventional smooth circular bend with a high-index-contrast rather than segmented corner mirrors [see Fig. 1(d)], our simulations showed that a conventional circular bend must be about 30% longer than the double mirror in order to match the performance. Also, Fig. 6 shows that increasing the dimension of the smooth circular bend even further, in terms of the radius of curvature, a , offers very little increase in transmission. For example, an additional 60% increase in the radius of curvature of the circular bend raises the transmission by only 0.7%. Since curved interfaces are generally harder to fabricate with conventional lithographic tools,

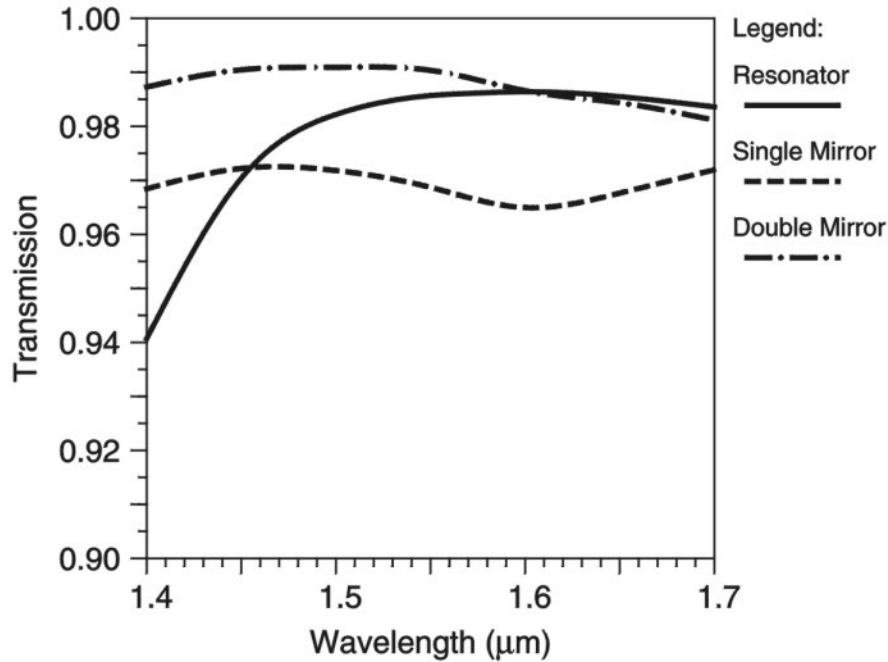


Fig. 7: Transmission spectrum of three bend structures: resonator bend, corner mirror bend, and double corner mirror bend.

fabricating ultra-small curve structures would have a greater practical difficulty than straight structures.

5 Comparative Discussion of the Wavelength Response of the Resonator and Mirror Bend Waveguides

Although, in this study, it was very difficult to completely isolate the individual roles of the different guiding mechanisms that lead to high transmission, it was possible to examine the relative merits of each through a careful variation and optimization of parameters. Figure 7 shows the optimum transmission curves for the two mirror designs compared to the resonator bend. The simple corner-mirror design maintains a relatively flat transmission at 96.6% over a bandwidth of more than 300 nm centered at $\lambda=1.55 \mu\text{m}$. The resonator bend does provide a somewhat higher transmission of 98.6% at $\lambda=1.55 \mu\text{m}$, but at the expense of a reduction in the flatness of the wavelength response. Finally, the double mirror structure provided the best performance, achieving a transmission of 99% at $\lambda=1.55 \mu\text{m}$, with a relatively flat wavelength response. The high performance from both mirror designs can be attributed to the combination of strong modal confinement due to high index contrast, phase-retardation at the inner wavefront, and total internal reflection(s) at the mirror facet(s).

Finally, one important criterion for an integrated optical device is its tolerance to fabrication error. An estimate of dimensional tolerance was performed on the mirrors and compared with that of the resonator bend. The width, d , and, incidentally, the overall bend factor, a , in the bend intersection region of each mirror design were varied $\pm 30 \%$, starting from the optimized design that produced maximum transmission at $\lambda=1.55 \mu\text{m}$. The input and output waveguide ports were kept constant at a width of $0.2 \mu\text{m}$. The resonator cavity side, a , was similarly varied $\pm 30 \%$ and the 45° cut depth, b , kept constant for comparison. This variation allowed us to examine the change in the

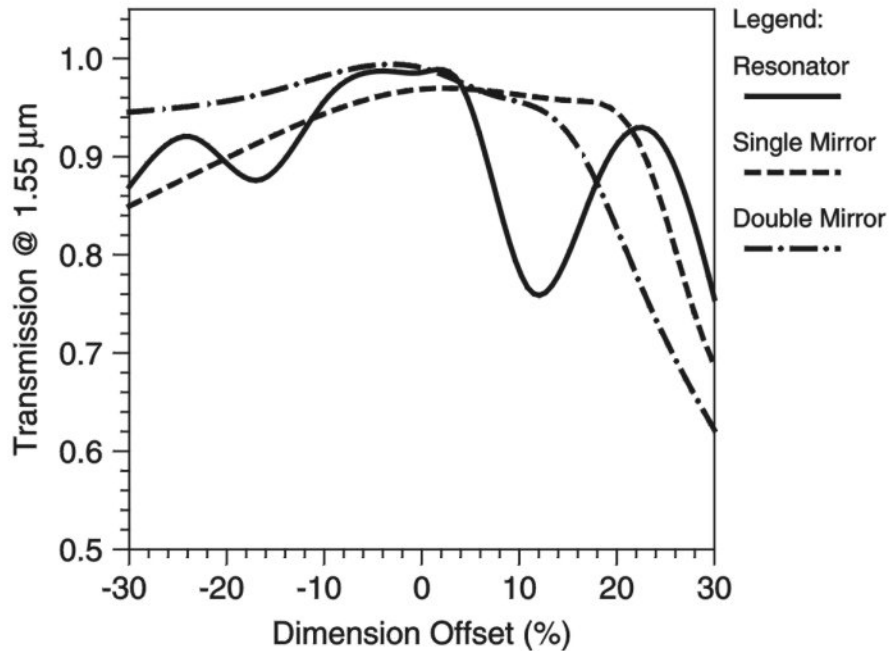


Fig. 8: Dimensional tolerance, at $\lambda=1.55 \mu\text{m}$, for the width, d , and bend factor, a , of the three bend structures presented in Fig. 7.

transmission as a function of dimensional error specifically on the device region, say, due to fabrication. As shown in Fig. 8, the corner mirror and the double mirror offer flatter responses and are more tolerant to dimensional error than the resonator. Therefore, it appears that, in terms of yield, the corner mirror might offer an interesting alternative to an abrupt 90° -bend design. The additional advantage of small device area would make it well suited to be a compact optical component in photonic integrated circuits.

6 Conclusion

We have made a comparative investigation of two high-index-contrast waveguide structures in order to determine which, if any, advantages are offered by each. The two structures include a resonator bend (Fig. 1(b)) and its variants, first described in Ref. [10], and a corner mirror, such as that described in Ref. [5]. The mirror investigated here was specifically adapted to and designed for high-index contrast waveguide structures and then further modified to obtain a double mirror design. Simulation results involving a variation in the placement of the resonator indicate that cavity resonance is not the dominant mechanism in achieving high transmission in abrupt bends, a result in accord with the low resonator Q . Rather, their performance is strongly dependent on device geometry and, hence, index-guiding effects. Further the study shows that either a corner mirror or a double mirror, which utilizes guiding mechanisms, can produce an equivalent performance and have better dimensional tolerance. Although all of these designs can help obtain a nearly lossless transmission around an abrupt 90° -bend, the double mirror design offers comparatively high peak transmission and flat transmission response.

Acknowledgements

This research was supported in part by AFOSR Contract No. F49620-99-1-0038, and by a NIST Advanced Technology Program under NIST Cooperative Agreement No. 70NANB8H4018. The authors gratefully acknowledge many useful and informative discussions with Dr. Robert Scarmozzino, Ms. Hongling Rao, and Dr. Jerry Chen.